FULL PAPER

Large Multipurpose Exceptionally Conductive Polymer Sponges Obtained by Efficient Wet-Chemical Metallization

Markus Langner, Seema Agarwal, André Baudler, Uwe Schröder, and Andreas Greiner**

Exceptionally conductive (250 S cm^{-1}), very fast electrically heatable, thermally insulating, antimicrobial 3D polymeric sponges with very low density (≈30 mg cm^{-3}), superhydrophobicity, and high porosity, their method of preparation, and manifold examples for applications are presented here. The electrical heatability is reversible, reaching 90 °C with 4.4 W in about 19–20 s and cooling immediately on switching off the voltage. The sponges show high contact angles >150° against water on the sponge surface as well as inside the sponge. Water droplets injected into the sponges are ejected. A facile wet-chemical method established for macroscopic melamine–formaldehyde sponges is the key for the thorough in-depth surface metallization of the sponges. The coating thickness and uniformity depend on the metallization formulation, conditions of metallization, and the type of metal used. A scanning electron microscope is used for morphology characterization. A reduced metallization rate in air is highly critical for the in-depth uniform coating of metals. The resulting metallized sponges could be highly interesting for heating as well as insulation devices in addition to oil/water separation membranes.

1. Introduction

Complex polymer structures, such as porous cellular solids, offer unique properties for a variety of applications.[1] Open cellular solids, also assigned as sponges, are of particular interest due to their excellent dimensional stability and open structure. Sponges are omnipresent in nature, predominantly in the marine environment,[2] and as polymeric materials in a variety of technical applications.[3] In contrast to polymer foams, sponges are 3D architectures that are made of interconnected fibrous segments. Sponges are typically highly porous and easily permeable by gases. Metallization of such sponges could give novel polymer/metal composites with highly interesting properties for a variety of applications, e.g., electrodes in fuel cells, membranes, filtration, thermal insulation, heating, ultralight constructions, and catalysis. Well-established metallization techniques for polymer materials include physical or chemical vapor deposition and galvanization.[4] These techniques are not suitable for achieving high conductivities by the metallization of macroscopic polymer sponges due to their complex 3D structure. The in-depth import of metals inside the pores of sponges and the formation of fully covered metal layers on the polymer fibrous segments are particular problems. A method of choice could be wet metallization, also assigned as electroless plating. There are some reports on wet metallization of porous polymer surfaces following different concepts. For example, gold coating of electrospun poly(methyl methacrylate) nonwovens was achieved by wet deposition of gold nanoparticles (NPs), which yielded conductivities up to 930 S cm^{-1}.[5] Here, copper would be more appropriate for many applications. Major pathways for copper plating of polymers are based on the treatment with copper salts and formaldehyde.[6] Wet chemical deposition of copper, for example, was achieved by treatment of an open-cell polyurethane sponge with $CuSO_4$ and formaldehyde under basic conditions using $PdCl_2$ as an activator.[7] Plasmonic copper nanoparticle coatings were prepared on silanized glass slides following an elegant approach also using $CuSO_4$ and formaldehyde, but gold as seed.[8] A number of efforts were undertaken using ultrasound for fast electroless plating.[9] However, ultrasound-assisted electroless plating required careful adjustment of the ultrasound frequency in order to avoid the pitting of the metal surface due to microjetting, which could also be a major problem in the absence of ultrasound due to evolving hydrogen bubbles.[10] The importance of the quality of the metal layer obtained by electroless plating on polymer substrates corresponds directly with their electrical properties. Broken and grainy metal layers or pitted surfaces will reduce their electrical conductivity significantly. However, nickel electrodes were produced with polyurethane foams under suitable plating conditions.[11] The polyurethane foams served as sacrificial templates. As a result, highly conductive nickel sponges with high porosities of up to 98% and pore sizes of several

M. Langner, Prof. S. Agarwal, Prof. A. Greiner
Macromolecular Chemistry II
University of Bayreuth and Bayreuth Center for Colloids and Interfaces
Universitätsstrasse 30, 95440 Bayreuth, Germany
E-mail: greiner@uni-bayreuth.de
A. Baudler, Prof. U. Schröder
Institute of Environmental and Sustainable Chemistry
Technische Universität Braunschweig
Hagenring 30, 38106 Braunschweig, Germany
E-mail: uwe.schroeder@tu-braunschweig.de

DOI: 10.1002/adfm.201502636

hundred micrometers were obtained which are used as cathode current collectors in metal hydride batteries.

Open cellular polymers with a spongy structure were prepared by a variety of different materials. Highly porous poly(styrene-co-acrylonitrile) (SAN) sponges, for example, were obtained by foaming with supercritical CO_2.[12] New ultraporous open cellular polymer sponges were recently reported, originating from dispersions of electrospun fibers.[13,14] A very versatile and also technically realized approach to highly porous polymer sponges was realized by microwave-assisted melamine-formaldehyde (MF) resin synthesis.[15] The MF sponges with apparent densities as low as 5.53 mg cm^{-3} were obtained depending on the use of emulsifiers. Electroless plating of MF sponges with $AgNO_3$ and $PdCl_2$ as activators yielded silver-coated sponges with good conductivity ($\sigma = 1.6 \times 10^3$ S m^{-1}) and good electronic shielding properties, but need surface modification of the sponge with chromium and tin salts.[16] Nevertheless, the realization of dense metal layers on MF sponges and in-depth penetration of reactants for homogeneous overall metallization of MF sponges of macroscopic dimensions remains a challenge and requires a careful balance of the plating conditions and choice of activators. The gain would be sponges with excellent conductivities which are of interest for manifold applications, e.g., as electrodes in microbial fuel cells. The efficiency of metals as electrodes in microbial fuel has been recently shown by our groups.[17]

We realized that a complete coverage of the MF sponge surface outside and inside of large polymer sponges by silver nanoparticles (AgNPs) as activators in combination with a slow metallization rate and high concentration of surfactant is crucial for obtaining a dense allover metal layer. This concept also prevents the massive evolution of hydrogen bubbles during metallization. The hydrogen evolved can prevent in-depth diffusion of fresh plating solution and, hence, provide an inhomogeneous coating. Following this concept, large exceptionally conductive (250 S cm^{-1}), very fast electrically heatable, thermally insulating MF sponges with low density (≈30 mg cm^{-3}), superhydrophobicity, and high porosity are presented by the metallization of the MF sponge with copper and silver. The effect of metallization formulation and plating conditions on metal coating thickness and uniformity was studied to provide a facile approach and interesting combination of properties in polymeric sponge by in-depth metallization.

2. Results and Discussion

2.1. Wet-Chemical Deposition of Copper and Silver on MF Sponges

Homogeneous wet metallization of MF sponges in order to achieve high conductivity was accomplished by successive treatment with poly(4-vinyl-pyridine) (P4VP), AgNP and, finally, by silver or copper plating solutions, following the scheme shown in **Figure 1**. First, MF sponge (MFS-1) was pretreated by a methanolic solution of P4VP to form a ligand containing surface on the sponge fibers. For surface activation and successful ligand layer formation, only a monolayer of P4VP is needed, but thicker layers do not harm the NP deposition. The treatment with P4VP requires only a low concentration of 6.6 mg mL^{-1} P4VP in methanol. This layer formation is followed by treatment with a dispersion of AgNP (see Supporting Information Figure S1 for AgNP size). The NP loading also can be done in situ via reduction of silver salt on the surface of the sponge fibers, but the control of size and shape of the in situ deposed NPs is a challenge. Preproduction of NPs provide better control over morphology of NPs. In this way, NPs of different size and shape can be obtained. To achieve a homogeneous deposition of metal, small AgNP (≈8 nm) were applied to guarantee a dense NP loading on the P4VP-coated sponge MFS-2 surface and to achieve a localized, catalytic, and very reactive nucleation site for the electroless deposition of copper in the next step.

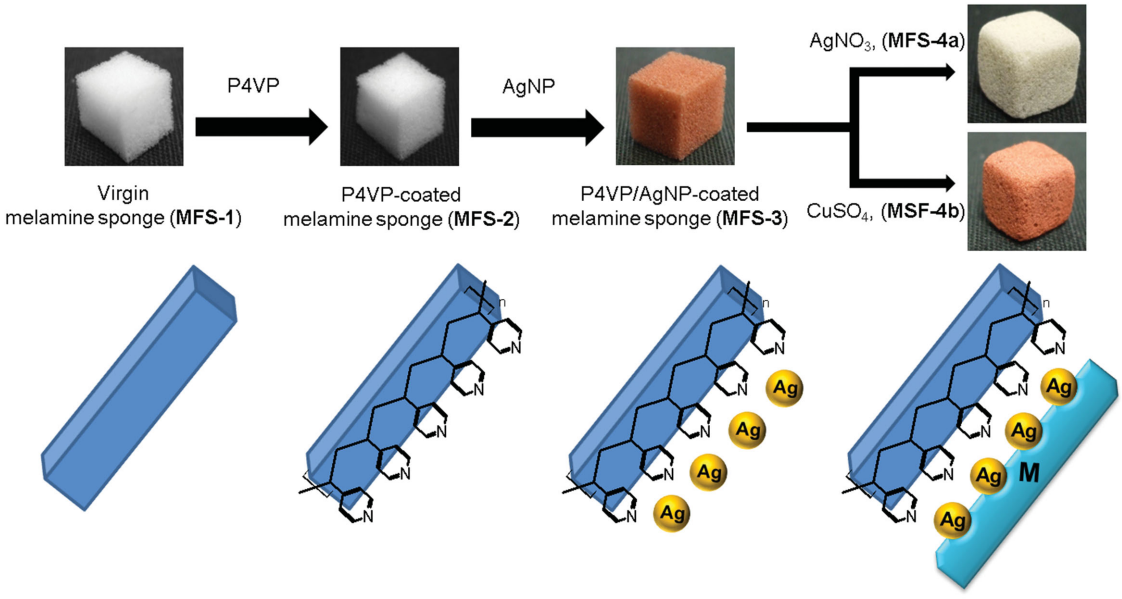

Figure 1. Schematic drawing of the metallization of MF sponges.

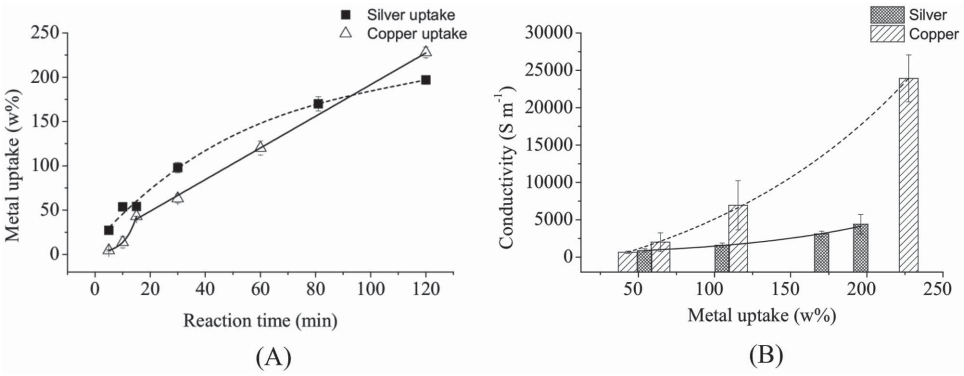

Figure 2. Weight gain of MFS-4a and MFS-4b due to A) metal uptake by MFS-3 versus reaction time for silver and copper and B) correlation of electrical conductivity with metal uptake.

During Ag deposition, NPs act as a seed for growth upon contact to the metallization solution. The idea behind this was that at a dense NP loading the necessary growth of particle to form a conductive metal layer is small. Without NP the Ag deposition occurs only randomly and a conductive layer is formed only with a higher amount of Ag than by using AgNP. At the copper deposition, the AgNPs catalyze the formaldehyde oxidation and according to this the copper deposition at the substrate. After covering of the AgNPs with copper, this acts as the catalyst and the autocatalytic copper deposition is started. The observed weight gain after P4VP treatment was 3.2 ± 0.6 wt% and for AgNP treatment 1.6 ± 1.1 wt%. This shows that only a small amount of P4VP and AgNP was needed for the activation. The deposition of AgNP on the sponges caused a color change from white to brown, which remained even after intensive rinsing with water. The metallized sponge (MFS-4) became orange in color after the deposition of copper and turned white-gray after the deposition of silver. The progress of silver and copper deposition on sponges was monitored gravimetrically and by the increase in conductivity (**Figure 2**A,B). The metal deposition on sponges was accompanied by a gradual change in the morphology of the metal layer from an open granular to a closed dense layer, as observed by SEM (**Figure 3**A–H). Compact copper and silver layers were obtained with longer reaction times, as seen by cross-sectional cuts of the sponges (**Figure 4**A,B). In-depth homogeneous coating of copper on 3D sponge was an unsolved challenge due to the liberation of hydrogen gas. The wet metallization on thin 2D substrates and foams/sponges with large pores (0.2–0.4 mm) is trivial and very well documented in the literature. The plating rate for such substrates can be easily increased by higher temperatures or faster plating compositions. The same process cannot be easily transferred to the MF sponges with macroscopic dimensions and pores in the micrometer range. The liberated hydrogen gas during wet metallization of copper can plug the pores of the sponges and, thereby, prevents the penetration of the reaction mixture toward the core, leading to only incomplete coating. The small pores themselves only allow slow diffusion of reaction media through the sponge. This problem was overcome in the present work by the reduction of the reaction rate using a tartrate-based metallization solution and a moderate temperature (45 °C). Another important step was the use of an appropriate amount of poly-(ethylene glycol) (PEG) that acts as a surfactant and inhibitor to the copper deposition. This suppression of the copper deposition allowed the mass transport of reactants and products out of the copper pores and yields

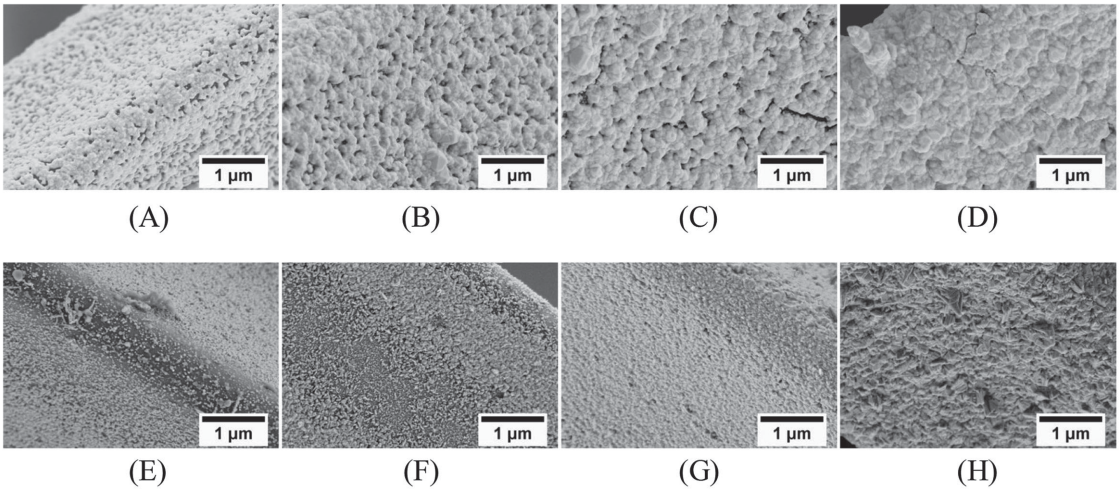

Figure 3. SEM images of MFS-4a surfaces after A) 5 min, B) 10 min, C) 15 min, and D) 30 min reaction time with a $AgNO_3$ solution and of MFS-4b surfaces after E) 5 min, F) 10 min, G) 15 min, and H) 30 min reaction time with a $CuSO_4$ solution.

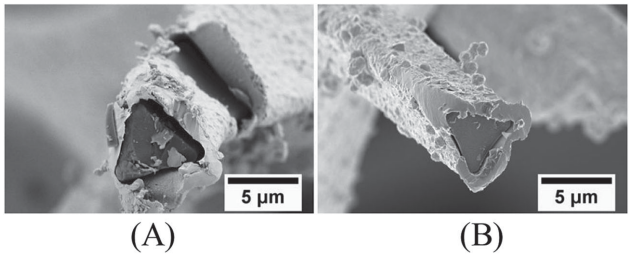

Figure 4. Cross-sectional SEM images of A) MFS-4a and B) MFS-4b after 120 min reaction time.

copper coatings free of pores.[18] An optimized concentration of 44 mmol L^{-1} provided dense in-depth metallization. With a concentration of 4.4 mmol L^{-1} only 50 nm copper particles were formed on the fibrous surface. The wet metallization of copper in air was also crucial in order to prevent the formation of upright standing copper plates which were otherwise formed under an argon atmosphere (see Supporting Information Figure S2). The in-depth deposition of copper was checked by mapping the copper thickness by SEM measurement on a cross-sectioned sponge. A 10 mm × 10 mm metallized sponge (MFS-4b) with 229% copper uptake after 2 h reaction time was cut from the middle and checked by SEM (**Figure 5**). The results clearly show the overall presence of copper in the cross-section. The copper thickness varies randomly from 450 to 850 nm, which provided sufficient homogeneity for excellent conductivity. In general, there is no thickness or weight limitation of metal loading on the sponges. Longer reaction times should lead to a copper layer in the µm range. But after ≈200+ wt% uptake of copper, we observed a beginning dendrite formation. These dendrites are mechanically unstable and not well attached to the surface. To avoid copper loss during mechanical stress, the reaction was stopped after ≈200 wt% loading. This dendrite formation can be avoided by the modification of the copper deposition solution, but this has to be developed in further research.

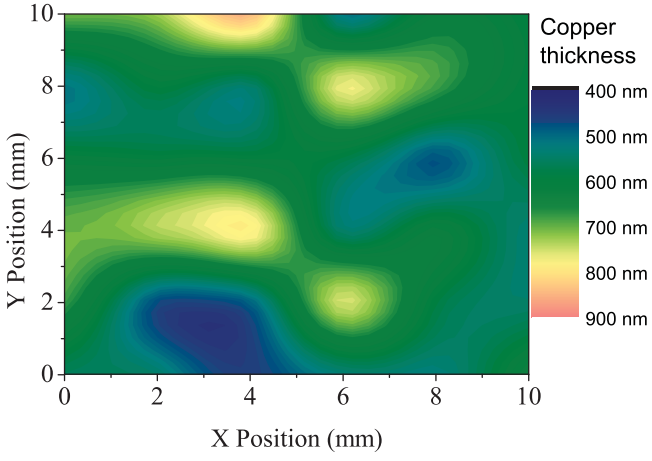

Figure 5. Proof of in-depth metallization of MFS-4b by SEM. Measurement of copper thickness from a cross-section of 1 cm^3 cubic MFS-4b from position 0;0;5 (*X*;*Y*;*Z*) to 10;10;5 (*X*;*Y*;*Z*) in 2 mm steps via SEM.

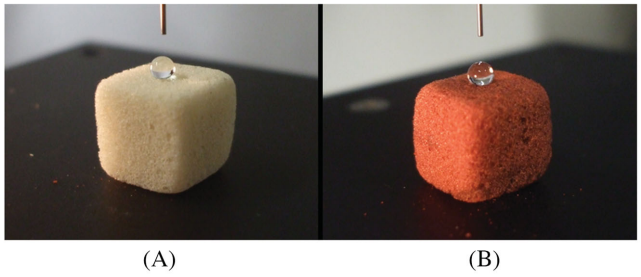

Figure 6. Photographs showing water droplets (8 µL) on A) silver-coated (MFS-4a) and B) copper-coated (**MFS4b**) MF sponge.

2.2. Properties of Sponges MFS-4a and MFS-4b

The metallized sponges showed low densities of 31 mg cm^{-3} (MFS-4a) and 35 mg cm^{-3} (MFS 4b) and high porosities of 99%. The metallization had no impact on the pore size and porosity of the sponges (see Supporting Information Figure S3 for pore size distribution measurement). After metallization, for example, the sponge MFS-4b showed nearly the same pore size distribution (75 ± 5 µm) as the untreated sponge, MFS-1 (81 ± 15 µm).

In contrast to the uncoated MF sponge (MFS-1), the metallized sponges (MFS-4a and MFS4b) showed high contact angles (MFS-4a 151° ± 3°; MFS-4b 152° ± 4°) against water (**Figure 6**), but no sliding of water droplets was observed even when the surfaces of the sponges were tilted to 180°. Superhydrophobic metal surfaces had been reported previously[19] and were attributed to fractal metal surfaces, which could also apply to the present sponges. The observation that water droplets injected into the sponges were ejected from the sponges rather rapidly (see Video in the Supporting Information) was very interesting and had, to the best of our knowledge, never been reported. By contrast, MFS-4a and MFS-4b were wetted by oil, which makes the sponges also promising membranes for oil/water separation in

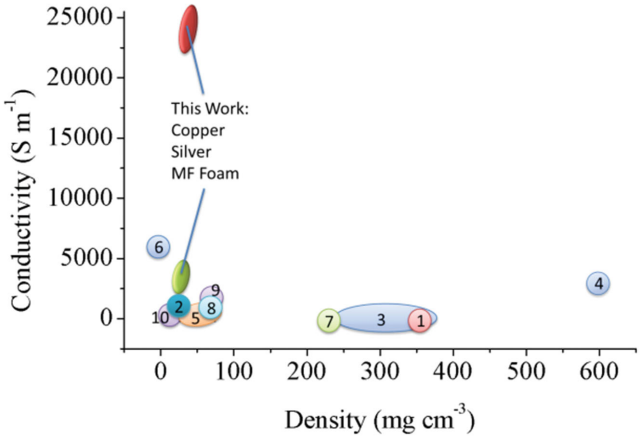

Figure 7. Ashby plot showing conductivities of sponges or foams made from different materials against their density. 1: graphene polymer composite,[21] 2: graphene aerogel,[23] 3: multiwall carbon nanotube (MWCNT) polyurethane composite,[26] 4: porous carbon,[27] 5: CNT and porous carbon,[27] 6: 3D graphene,[28] 7: polypyrrole polyurethane composite,[29] 8: polypyrrole poly(vinyl alcohol) composite,[30] 9: reduced graphene oxide,[31] and 10: CNT aerogel.[32]

the future. It is needless to say that copper- as well as silver-coated sponges are antimicrobial which will be discussed in detail in a separate contribution.

With the formation of a compact copper layer on the sponge fibers, the conductivity increased exponentially to a value of $\sigma = 2.4 \times 10^4$ S m^{-1} at an uptake of 228 ± 6 wt% of copper (Figure 2B). The final conductivity of MFS-4b is much higher than MFS-4a ($\sigma = 4.4 \times 10^3$ S m^{-1}, 197 ± 5 wt% of Ag). The difference in the conductivity of MFS-4a and MFS-4b is speculatively attributed to crystalline defects in the silver layer due to the metallization process, which were reported previously.[20] However, the conductivity of MFS-4a is still several magnitudes higher compared to graphite-modified polymer sponges (7 S m^{-1}) or sponges made of carbon nanotubes (CNTs) (59 S m^{-1}),[21,22] and is comparable to that of graphene aerogels (1×10^2 S m^{-1})[23] or graphene/poly(dimethyl siloxane) composites (1×10^3 S m^{-1}).[24] The conductivity of MFS-4b is many times higher than CNT and graphene-based polymer sponges and aerogels. A comparison of the conductivity of metallized MF sponges obtained in the present work in comparison to literature values based on carbon, graphene, conductive polymer-based composites, foams/sponges, and aerogels is shown as an Ashby plot in **Figure 7**. The copper-coated MFS-4b stands out for its exceptionally high conductivity ($\sigma = 2.4 \times 10^4$ S m^{-1}) and for very low density. Interestingly, the electrical conductivity of sponge MFS-4a was also high enough to operate a multiple light-emitting diode (LED) device in a sandwich setup (**Figure 8**A).

Sponge MFS-4a with 200 wt% uptake of Ag showed with dimensions of 25 mm × 5 mm × 50 mm with a fixed current significant electrical heating and cooling within a few seconds

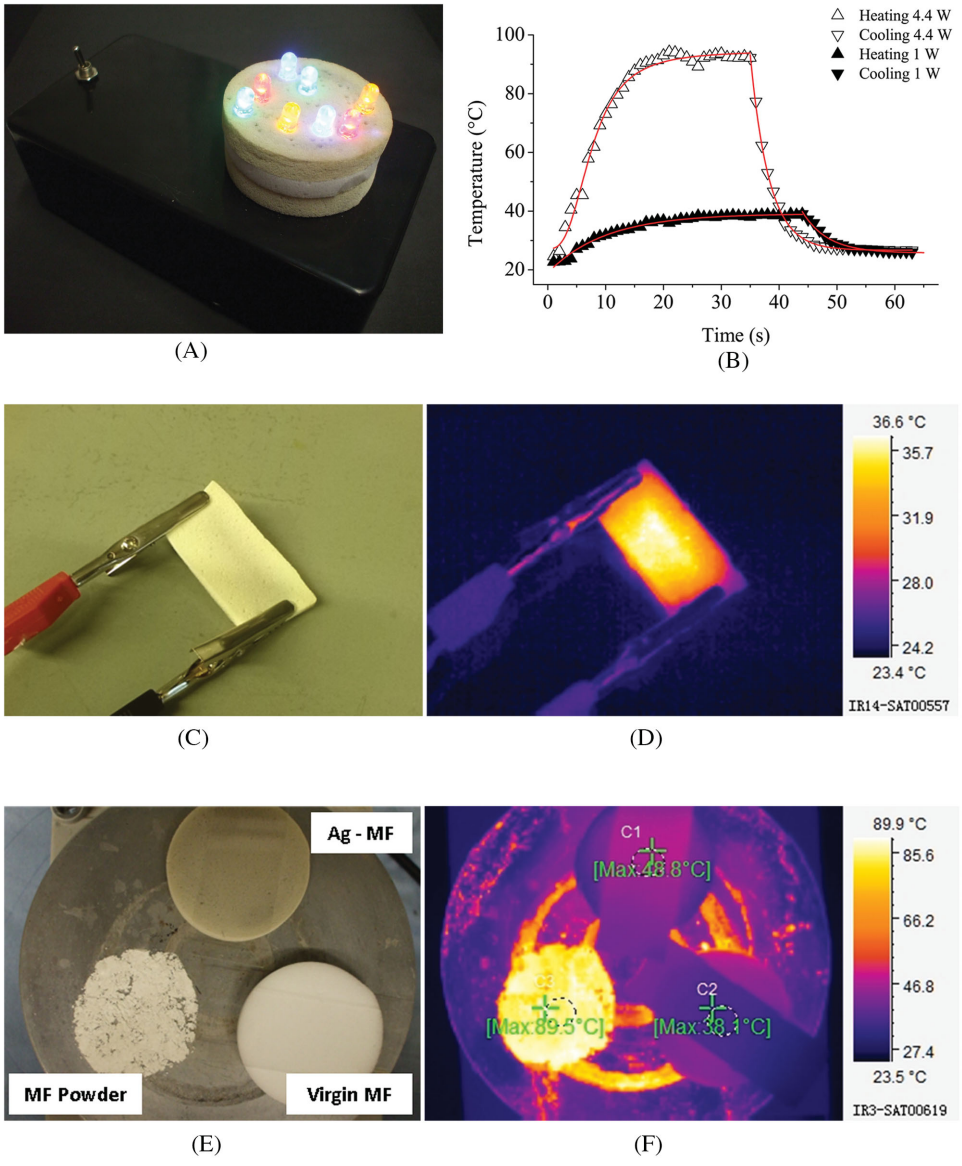

Figure 8. A) Photograph of LED sandwich setup of MFS-4a. B) Time–temperature plot of MFS-4a with current flow and after switching off the current. C,D) Photograph and infrared camera image of MFS-4a at a power of 1 W. Photograph of sponges MFS-1, MFS-4a, and ground MFS-1 on a heating plate at 100 °C and corresponding infrared camera image is shown in (E) and (F).

when the current was turned on-off (Figure 8B). Heat produced at the sponge by 4.4 and 1 W meant that it could be heated to 90 and 37 °C, respectively, in 19–20 s, as visualized by infrared camera (Figure 8C,D). Similar to other porous materials on aerogel basis,[25] MFS-4a also displayed heat insulating properties similar to the uncoated sponges (MFS-1) (Figure 8E,F). By contrast, a ground sample of MFS-1 showed no heat insulation (Figure 8F). The oxygen content of a 134 wt% copper-loaded sponge was determined via energy dispersive x-ray spectroscopy (EDX). The results show that nearly no oxygen is detectable. But for sponges with less copper content the amount of oxygen can be higher caused by higher surface roughness (see Supporting Information Figure S4 for EDX measurement). After metallization, the polymer template of the metallized sponges can be removed by heating them in air above 400 °C. We performed a TGA experiment where the sponges are heated to 500 °C and kept there for 30 min. The copper-coated sponge oxidized to copper oxide that was successfully reduced in an ethanol atmosphere at 400 °C. The Ag-coated sponge template is also removed with this procedure but the silver coating melted to droplets that are interconnected to the template structure. Both polymer-free metal sponges were very brittle and are damaged on touching with tweezers (see Supporting Information Figure S5 for SEM measurements).

3. Conclusion

Homogeneous deposition of AgNPs on MF sponges allowed the deposition of thick and persistent silver and copper layers. The critical factors for obtaining in-depth homogenous metallization of 3D sponges of macroscopic dimensions are the slow plating rate realized by low temperature and by the use of tartrate as a ligand, careful degassing, an optimum amount of PEG, and metallization in air. The metal-coated sponges showed exceptional electrical conductivities of up to $\sigma = 2.4 \times 10^4$ S m^{-1} and tolerated currents of up to 10 A. Without current flow, the sponges were thermal insulators, which makes them of particular interest as thermal devices. The large contact angles of the metallized sponges against water were an unexpected feature, which is of interest for oil/water separation. Water droplets injected into the core of metal-coated MF sponges were rapidly ejected, which should prevent unwanted water uptake and, thereby, fouling. Antifouling is also supported by the inherent antimicrobial properties of silver and copper. The concept applied for metallization could be transferred to many other porous systems and to other metals for the generation of various highly functional materials with numerous applications.

4. Experimental Section

Materials: $AgNO_3$ (p.A., Acros), α-D (+) glucose (99+%, Acros), D/L tartaric acid anhydrous (>99%, Fluka), NaOH (≥98%, Sigma-Aldrich), NH_4OH (24 wt%, Sigma-Aldrich), ethanol (absolute, 99.9%, VWR), sodium citrate (98%, Acros), $NaBH_4$ (≥96%, Fluka), $CuSO_4{\cdot}5H_2O$ (99+%, Acros), potassium sodium tartrate tetrahydrate (Acros), formaline (37 wt%,), PEG 400 (Fluka), pyridine (anhydrous, 99.8%, Aldrich), P4VP (M_w = 160 k, Aldrich), MF sponge (MFS-1) (Flexolan e.K, Germany), and water (Mili Q plus freshly prepared) was used as received. Methanol (tech.) was distilled before use.

Preparation of Silver Nanoparticle Suspension: AgNPs (8 nm) were prepared using a procedure in the literature with slight variations.[33] In brief, an amount of 42 mg (0.247 mmol) $AgNO_3$ and 65 mg (0.252 mmol) sodium citrate were dissolved in 1000 mL water in a 1000 mL Schott flask and stirred for 1 min. Subsequently, 0.55 mg (0.015 mmol) $NaBH_4$ dissolved in 3 mL water was injected via pipette into the solution and stirring was continued for another 2 min. The resulting AgNP suspension was stored at 4 °C until use.

Surface Modification of MFS-1 with P4VP: The P4VP (100 mg) was dissolved under stirring in 15 mL methanol (6.6 mg mL^{-1}). An MFS-1 cube (10 mm × 10 mm × 10 mm) was immersed into the solution and stirred for 1 min. The sponge was placed on filter paper and the methanol was pressed out of the sponge until no further liquid was observed on fresh filter paper. After this, the P4VP-coated sponge was dried in vacuum at 80 °C and designated as MFS-2.

Loading of MFS-2 with AgNP: MFS-2 was immersed in 10 mL of a 0.2×10^{-3} M AgNP dispersion. After this, the solution was degassed twice at 1 mbar until the solution began to boil. The sponge was left in AgNP dispersion for 24 h under shaking. The AgNP suspension was renewed every 24 h for four times until the sponge was fully covered with NPs. The resulting P4VP/AgNP-coated sponge is designated as MFS-3.

Wet-Chemical Deposition of Silver on MFS-3: The Ag deposition formulation was made according to the literature reported previously, with some variations.[34] In brief, the Ag deposition suspension was prepared using three different solutions in different steps:

1. Solution 1 was prepared by dissolving 5 g $AgNO_3$ in 100 mL of water.
2. Solution 2 was prepared by dissolving 0.05 g NaOH and 8.2 mL of ammonia solution (25 wt%) in 100 mL of water.
3. Solution 3 was prepared by dissolving 0.4 g D/L tartaric acid, 2.75 g α-D (+) glucose, and 10 mL of ethanol in 100 mL of water.

In order to achieve metallization, 1 mL of Solution 1 was mixed with 1 mL of Solution 2 and combined with 2 mL of Solution 3 in a 10 mL glass flask with a magnetic stirring bar. MFS-3 was placed in the flask, shaken, and carefully degassed with heating to 50 °C. Sponge samples were taken at different time intervals and rinsed with water. The wet sponges were placed on filter papers for predrying, followed by drying at 80 °C in vacuum to yield silver-coated MFS-4a.

Wet-Chemical Deposition of Copper on MFS-3: The copper deposition solution was prepared as reported previously with modifications.[35] In brief, an amount of 2.5 g (10 mmol) $CuSO_4{\cdot}5H_2O$ was dissolved in 100 mL water in a 250 mL volumetric flask, followed by dissolution of 6.25 g (22 mmol) potassium sodium tartrate tetrahydrate. Subsequently, 2.5 g (62 mmol) NaOH, 500 mg (11.35 mmol) PEG, 15 mg pyridine, and 7.5 mL formaline (37%) were dissolved in the solution. The flask was filled up to 250 mL and the solution was homogenized by shaking.

For the deposition of copper on MFS-3, 20 mL of the solution prepared above was poured into a 40 mL glass flask which had a magnetic stirring bar and a venting hole in the lid. MFS-3 was placed in the flask and the same procedure as for Ag deposition was applied at a water bath temperature of 45 °C. The copper-coated sponges are designated as MFS-4b.

SEM Measurements: A LEO 1530 SEM wit Oxford 6901 EDX detector was used to obtain images of the surface of the silver and copper coatings prepared on the sponges and to measure EDX spectra. For SEM, the samples were covered with 2 nm of platinum via a sputter coater 208 HR from Cressington; for EDX, the samples were uncovered. The samples were glued onto sample holders with water-based conductive carbon glue prepared in our lab.

Analysis of Resistivity of MFS-4: In order to analyze resistivity, MFS-4 was pressed between two parallel copper plates (each 1 mm thick) that were connected to a Keithley 2420 High-Current Source Meter. Prior to measurement, the system resistivity of the wires and plates were collected and subtracted from the measured values of the system and

the sponges. Three samples were measured from all three sides for every data point and a mean value was calculated.

Current Source Heating and Isolation Measurement: A DF-3010 lab power source with a fixed current of 5.2 A (1 W) and 10.34 A (4.4 W) was used for heating up the metal-covered sponge. An MR 3001 K magnet stirrer with hotplate from Heidolph was used to measure the isolation behavior of metal-coated, uncoated (MFS-1), and ground sponges. The hotplate was set to 100 °C. The weight of the ground sponge was the same as that of the unground sponge. The temperature of the sponges from both tests was measured with a SAT HotFind infrared camera from ICOdata GmbH with an emission coefficient set to 1.0.

LED Lightning Device: A sandwich of two sponges (MFS-4a) was used to light up the LEDs. An array of 8 AA alkaline batteries that delivered 12 V was used to connect one sponge positive and one negative. The wires of the LEDs (12 V, Winger) were cut so that one was isolated and only reached the lower level sponge. The other wire was cut shorter and was insulated so that it could only be connected to the upper level sponge. The same procedure was applied to connect the batteries to the sponges.

Contact Angle Measurement: The advancing contact angles were measured at 20 °C using a drop shape analyzer DSA25S from Krüss. Drop size was controlled to 8 µL. The Young–Laplace fit was used with ADVANCE software 1.1.0.2 from Krüss for the calculations.

Pore Size Determination: The pore size distribution of MFS-1 and MFS-4b was measured with a pore size meter (PSM 165/H) from Topas with Topor as the test liquid.

TGA Measurement: The thermal degradation of the metallized sponges was performed with a Libra F1 Tg-209 TGA from Netsch at 10 K min^{-1} from 20 to 500 °C with a 30 min plateau at 500 °C at an airflow of 20 mL min^{-1}.

Supporting Information

Supporting Information is available from the Wiley Online Library or from the author.

Acknowledgements

The authors would like to thank DFG for financial support.

Received: June 28, 2015
Revised: August 17, 2015
Published online: September 15, 2015

[1] S. P. Leys, A. Hill, *Adv. Mar. Biol.* **2012**, *62*, 1.
[2] M. A. Becerro, M. A. Uriz, M. Maldonado, X. Turon, *Advances in Marine Biology*, Elsevier, London, UK **2012**.
[3] M. Paunovic, M. Schlesinger, D. D. Snyder, in *Modern Electroplating*, 5th ed. (Eds: M. Schlesinger, M. Paunovic), John Wiley & Sons, Hoboken, NJ, USA **2010**.
[4] D. Eaves, *Handbook of Polymer Foams*, Smither Rapra Press, Acron, OH, USA **2004**.
[5] S. Nakahara, Y. Okinaka, *Ann. Rev. Mater. Sci.* **1991**, *21*, 93.
[6] G. Han, B. Guo, L. Zhang, B. Yang, *Adv. Mater.* **2006**, *18*, 1709.
[7] Q.-H. Tian, X.-Y. Guo, *Trans. Nonferrous Met. Soc. China* **2010**, *153*, s283.
[8] M. D. Susman, Y. Feldman, A. Vaskevich, I. Rubinstein, *Chem. Mater.* **2012**, *24*, 2501.
[9] A. J. Cobley, T. J. Mason, V. Saez, *Trans. Inst. Met. Finish.* **2011**, *89*, 303.
[10] Y. S. Park, M. H. Kim, S. C. Kwon, *Surf. Coat. Technol.* **2002**, *20*, 245.
[11] S. Inazawa, A. Hosoe, M. Majima, K. Nitta, *Sci. Technol. Rev.* **2010**, *71*, 23.
[12] L. Kyung-Nam, H.-J. Lee, J-H. Kim, *Polym. Int.* **2000**, *49*, 712.
[13] Y. Si, J. Yu, X. Tang, J. Ge, B. Ding, *Nat. Commun.* **2014**, *5*, 5802.
[14] G. Duan, S. Jiang, V. Jérôme, J. H. Wendorff, A. Fathi, J. Uhm, V. Altstädt, M. Herling, J. Breu, R. Freitag, S. Agarwal, A. Greiner, *Adv. Funct. Mater.* **2015**, *25*, 2850.
[15] D. Wang, X. Zhang, S. Luo, S. Li, *Adv. Mater. Phys. Chem.* **2012**, *2*, 63.
[16] Y. Xu, Y. Li, W. Xu, J. Bao, *J. Mater. Sci.: Mater. Electron.* **2015**, *26*, 1159.
[17] A. Baudler, I. Schmidt, M. Langner, A. Greiner, U. Schröder, *Energy Environ. Sci.***2015**, *8*, 2048.
[18] X. Wang, Q. Shen, Z. Shu, *Int. J. Electrochem. Sci.* **2013**, *8*, 4670.
[19] K. Liu, L. Jiang, *Nanoscale* **2011**, *3*, 825.
[20] L. Lu, Y. Shen, X. Chen, L. Qian, K. Lu, *Science* **2004**, *304*, 422.
[21] S. J. Woltornist, J. M. Y. Carrillo, T. O. Xu, A. V. Dobrynin, D. H. Adamson, *Macromolecules* **2015**, *48*, 687.
[22] X. Gui, A. Cao, J. Wei, H. Li, Y. Jia, Z. Li, L. Fan, K. Wang, H. Zhu, D. Wu, *ACS Nano* **2010**, *4*, 2320.
[23] M. A. Worsley, P. J. Pauzauskie, T. Y. Olson, J. Biener, J. H. Satcher, T. F. Baumann, *J. Am. Chem. Soc.* **2010**, *132*, 14067.
[24] H. M. Kim, H. S. Kim, S. Y. Kim, J. R. Youn, *e-Polymers* **2015**, *15*, 111.
[25] Z. Chen, W. Ren, L. Gao, B Liu, S. Pei, H. M. Cheng, *Nat. Mater.* **2011**, *10*, 424.
[26] A. Baltopoulos, N. Athanasopoulos, I. Fotiou, A. Vavouliotis, V. Kostopoulos, *eXPRESS Polym. Lett.* **2013**, *7*, 40.
[27] M. A. Worsley, S. O. Kucheyev, J. H. Satcher, A. V. Hamza, T. f. Baumann, *Appl. Phys. Lett.* **2009**, *94*, 73115.
[28] K. Chen, L. Chen, Y. Chen, H. Bai, L. Li, *J. Mater. Chem.* **2012**, *22*, 20968.
[29] Y. Fu, R. A. Weiss, P. P. Gan, M. D. Bessette, *Polym. Eng. Sci.* **1998**, *38*, 857.
[30] H. Bai, C. Li, F. Chen, G. Shi, *Polymer* **2007**, *48*, 5259.
[31] Z. Xu, Y. Zhang, P. Li, C. Gao, *ACS Nano* **2012**, *6*, 7103.
[32] X. Liu, H. Li, Q. Zeng, Y. Zhang, H. Kang, H. Duan, Y. Guo, H. Liu, *J. Mater. Chem.* **2015**, *3*, 11641.
[33] C. Liu, B. Li, *Anal. Bioanal. Chem.* **2011**, *401*, 229.
[34] L. Lili, Y. Dan, W. Le, W. Wie, *J. Appl. Polym. Sci.* **2012**, *124*, 1912.
[35] F. Hanna, Z. A. Hamid, A. A. Aal, *Mater. Lett.* **2003**, *58*, 104.